Bulletin of the Seismological Society of America, Vol. 93, No. 4, pp. 1531–1541, August 2003

Characteristics of Small-Scale Heterogeneities in the Hidaka, Japan, Region Estimated by Coda Envelope Level

by Taka'aki Taira and Kiyoshi Yomogida

Abstract We estimated the spatial distribution of small-scale heterogeneities as anomalous amplification of coda level in the Hidaka, Japan, region. We analyzed 2768 seismograms in a frequency range of 1–32 Hz for 24 earthquakes recorded at 62 stations. First, we estimated the site effect of each station, using the coda normalization method with regional earthquake data of large epicentral distances. All the data processing was done after the correction of this site effect. Next, we determined coda amplitude factor (CAF), that is, the amplitude ratio of coda waves on each source–station pair relative to the averaged coda amplitude over stations, for earthquakes inside the region. We found systematic spatial variations of CAF, implying the existence of localized heterogeneities. At frequencies lower than 2 Hz, the CAF is relatively large in the west of the Hidaka Mountains, implying the possibility of strong heterogeneities with a scale of 0.6–1.3 km there. In a high-frequency range (>16 Hz), CAF values are large on paths crossing the Hidaka Mountains. From the corresponding lapse time of coda (65 sec), there may be a zone of concentrated heterogeneities beneath the Hidaka Mountains at the depth of 100–120 km.

Introduction

Small-scale heterogeneous structures in the Earth are recognizable by excitation of incoherent coda waves and attenuation of high-frequency seismic waves. Based on the single backscattering model for a stationary random medium (i.e., heterogeneities distributed uniformly in space), Aki (1969) and Aki and Chouet (1975) quantitatively estimated small-scale heterogeneities from *S* coda wave envelopes. Much progress has been made in this research field since then, as summarized by Sato and Fehler (1998). One promising recent research movement is that the distribution of small-scale heterogeneities has been gradually revealed, using dense seismic networks. For example, Nishigami (1991, 1997), Revenaugh (1995), and Matsumoto *et al.* (1998, 1999) estimated the spatial distribution of heterogeneities in each active seismic area from high-frequency coda waves.

The structure of the Hidaka Mountains in Hokkaido, Japan, suggests that the crust of the Kurile Outer Arc has overthrusted the crust of the Northern Honshu Outer Arc due to their collisional movement (e.g., Moriya *et al.*, 1998). There are several active seismic zones around the Hidaka region. The maximum stress axis estimated from focal mechanisms of earthquakes beneath the Hidaka Mountains is similar to that estimated from earthquakes in the subduction zone of the Pacific plate in the south (Moriya *et al.*, 1997). On the other hand, earthquakes with other kinds of focal mechanisms exist just beneath high peaks of the Hidaka Mountains. This suggests that a complex stress field is produced there by the overthrust structure and by the collision in the root of the Hidaka Mountains with the convex part of the subducting Pacific plate as an arc–arc junction.

Since the spatial variation of stress depends strongly on the distribution of heterogeneities, it is important to investigate the detailed characteristics of heterogeneous structures in order to understand the process of such inland earthquake occurrence and the nature of the subducting plate in this region. Seismic tomography should be a very useful technique for large-scale heterogeneities (e.g., Iyer and Hirahara, 1993), and tomographic studies were done in this region (e.g., Katsumata *et al.*, 1999). Unfortunately, small-scale heterogeneities from high-frequency seismic waves have not been investigated quantitatively yet, particularly in a deterministic manner.

In this study, we shall investigate small-scale heterogeneities beneath the Hidaka Mountains, using coda envelopes of high-frequency (>1 Hz) seismic waves observed by a dense seismic array. In order to obtain the spatial variation of small-scale heterogeneities in this tectonically active area, we follow the two major steps: (1) estimating site effects from regional earthquakes with an epicentral distance of 200 km, and (2) correcting these site effects and estimating coda amplitude from local earthquakes. While the previous studies each observed the coda level normalized by its maximum in an *a priori* manner, this study defines coda levels to be mapped into heterogeneities as their amplitudes after correcting the site effect.

Data

Observed seismograms show extremely complex features in a frequency range of higher than 1 Hz. In order to evaluate the character of high-frequency seismic waves quantitatively, it is essential to use dense seismic networks. In the Hidaka region, the Research Group of the Hidaka Collision Zone has operated a dense seismic network since 1999 (Katsumata *et al.*, 2001a). The Institute of Seismology and Volcanology, Hokkaido University, also carried out routine observations with many stations in this area. Figures 1 and 2 show 62 stations and the epicenters of 24 earthquakes used in this study, respectively. Most of the stations were equipped with three-component velocity seismometers with the natural frequency of 1 Hz. Seismograms were recorded at 100 Hz sampling frequency. Hypocentral parameters were determined by the Institute of Seismology and Volcanology, Hokkaido University, as listed in Table 1.

As mentioned in the Introduction, we shall first determine the site amplification factor of each station from seismograms for regional earthquakes, sufficiently far from our studied area (epicentral distance $>$ 200 km). In contrast, coda levels related to the distribution of small-scale heterogeneities in this area are estimated for local earthquakes within the studied area, as shown in Figure 2. Figure 3 shows sample seismograms for regional and local earthquakes.

In this study, we analyze seismograms of six frequency bands with the centers of 1, 2, 4, 8, 16, and 32 Hz and bandwidths of 0.25, 0.5, 1, 2, 4, and 8 Hz, respectively. In each frequency band, seismograms are first bandpass filtered by a butterworth filter of four-pole octave width. A cosine taper time window is used to specify the lapse time of coda throughout this study.

Relative Site Amplification Factor

Assuming a homogeneous distribution of heterogeneities and a theory based on single scattering only, Aki and Chouet (1975) described the time- and frequency-dependent amplitude of coda waves as

$$A_{ij}(f, t) = S_i(f) \cdot G_j(f) \cdot C_{ij}(f, t), \qquad (1)$$

where $A_{ij}(f, t)$ indicates the amplitude of coda waves for the ith earthquake at the jth station for the lapse time t of the

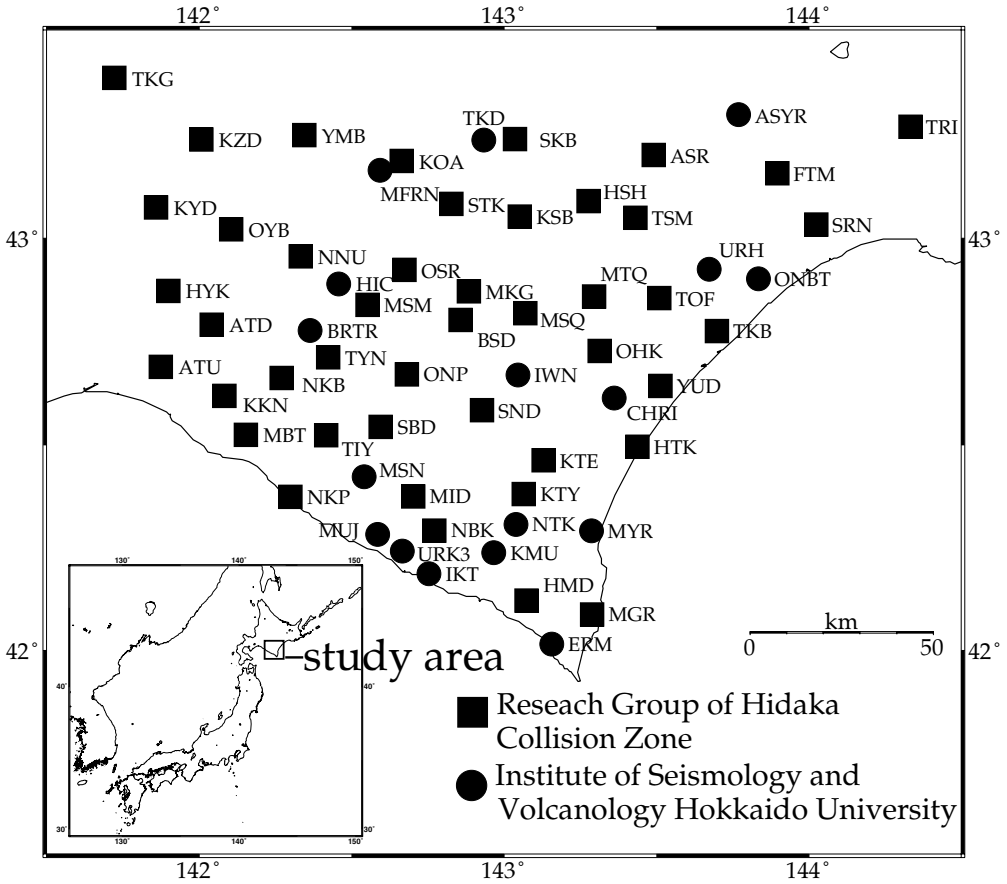

Figure 1. Distribution of stations used in this study. Squares indicate the stations of the Research Group of the Hidaka Collision Zone, and circles those of the Institute of Seismology and Volcanology, Hokkaido University.

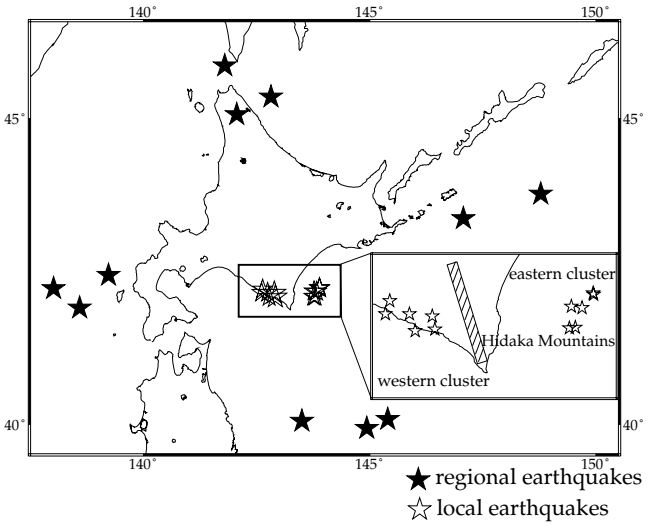

Figure 2. Epicenter distribution of earthquakes analyzed in this study. Solid stars indicate regional earthquakes, while local earthquakes are indicated by stars.

frequency f. $S_i(f)$ is the source term of the ith earthquake, $G_j(f)$ is the site term of the jth station, and $C_{ij}(f, t)$ is the path term related to the coda decay curve. To estimate the site term $G_j(f)$ of the jth station, we take the amplitude ratio of $A_{ij}(f, t)$ at the same lapse time t for the ith earthquake to the averaged coda amplitude $\tilde{A}_i(f, t)$ over all the stations:

$$\frac{A_{ij}(f, t)}{\tilde{A}_i(f, t)} = \frac{S_i(f) \cdot G_j(f) \cdot C_{ij}(f, t)}{S_i(f) \cdot \tilde{G}(f) \cdot \tilde{C}(f, t)} \simeq \frac{G_j(f)}{\tilde{G}(f)} \equiv \mathrm{RSAF}_{ij}(f), \quad (2)$$

$$\mathrm{RSAF}_j(f) \equiv \frac{1}{N} \sum_{i=1}^{N} \mathrm{RSAF}_{ij}(f), \quad (3)$$

where $\tilde{G}(f)$ is the average of all the site terms. The implicit assumption in equation (2) is that the coda decay curve $C_{ij}(f, t)$ is grossly independent of source–station pairs, that is, $C_{ij}(f, t) \simeq \tilde{C}(f, t)$, proposed by Aki (1969) and supported by numerous observations since then, particularly on the coda part of later than twice the travel time of the direct S wave, due to the averaging effect of heterogeneities over a given area (e.g., Sato and Fehler, 1998). With increasing lapse time, the nonspherical radiation pattern from the source does not become effective on seismograms (Sato and Fehler, 1998) and the source term $S_i(f)$ can be considered to be isotropic. The ratio in equation (2) means the relative site amplification factor of the jth station, so hereafter we shall call the ratio $\mathrm{RSAF}_j(f)$.

Before using equation (2), we need to confirm that a common decay curve of coda or $C_{ij}(f, t) \simeq \tilde{C}(f, t)$ can be applied to our data set. Assuming that coda waves from regional earthquakes are composed of single backward-scattered body waves, $C_{ij}(f, t)$ is expressed as

$$C_{ij}(f, t) \propto t^{-1} \exp\left(-\frac{\pi f t}{Q_c(f)}\right), \quad (4)$$

where $Q_c(f)$ is the quality factor of coda waves (Aki and Chouet, 1975). This representation of equation (4) satisfies the earlier assumption of $C_{ij}(f, t)$ in equation (2).

We evaluate the RSAF(f) of each station by using 12 regional earthquakes, as shown in Figure 2. These earthquakes were selected to cover nearly all the directions from the region in order to avoid any strong biases of directivity in site effects or distribution of heterogeneities. These coda waves are considered as scattered waves by heterogeneities in a much larger area than a region covered with the seismic array, probably over the entire Hokkaido region and the depth down to the whole lithosphere, so that any localized heterogeneities, which will be discussed later in this study, should be smoothed out in these coda waves. We estimated coda decay curves or the decay rate of coda, Q_c^{-1}, by the maximum likelihood method (Takahara and Yomogida, 1992). We analyzed the coda part with lapse time greater than twice the S-wave travel times for the RSAF (so as for CAF in the next section) in this study (e.g., starting time: in the case of regional earthquakes, 196 sec; 54 sec for local earthquakes), and the time window is 20 sec (Figs. 3 and 4).

Figures 5 and 6 show Q_c^{-1} values for all the stations and all the regional earthquakes, respectively. Q_c^{-1} values at a given frequency band are nearly constant among regional earthquakes as well as among stations. Figure 7 shows that Q_c^{-1} values are also nearly the same among components. Mean values of Q_c^{-1} are 7.1×10^{-3} and 1.3×10^{-3} for center frequencies of 1 and 8 Hz. These features indicate that decay properties of coda waves are independent of not only hypocentral locations of earthquakes but also station locations, supporting the applicability of equation (4) and the use of equation (2) with our data.

Since we have shown the validity of equation (2) in our data, we estimate RSAF(f) as the site effect at each station, normalized by the average coda amplitude over all stations. Figure 8 shows the distribution of RSAF(f) values in the transverse component in our study area at each frequency band. At Quaternary sedimentary sites (e.g., YUD and OHK), site amplification factors are larger (>1.5 times) than the average. In contrast, the RSAF(f) at Hidaka metamorphic rock sites (e.g., ERM and HMD) is generally small. According to Phillips and Aki (1986), coda site amplification factors reflect surface geology such as sediment and granite, at least in a low-frequency range (<4 Hz).

Anomalous Amplification of Coda Level

If heterogeneities take a spatially stationary distribution, observed coda levels after the site correction of the RSAF,

Table 1
Hypocentral Parameters of Earthquakes

Date (YY-MM-DD)	Time (JST)	Latitude (°)	Longitude (°)	Depth (km)	Magnitude
		Regional Earthquakes			
99-07-20	23:53:28:568	43.13662N	136.71611E	392.735	5.2
99-07-24	10:42:32.662	43.41226N	147.07026E	−0.033	5.6
99-07-27	14:30:18.587	39.93779N	144.93652E	84.298	6.1
99-08-06	17:29:50.907	45.06716N	142.05887E	331.140	5.0
99-09-23	02:35:28.063	45.33954N	142.81912E	357.318	6.3
99-09-27	08:38:36.101	43.80692N	148.78010E	73.864	6.4
99-10-03	06:08:37.978	40.05653N	143.49801E	104.232	6.3
99-10-15	22:49:46.636	41.95575N	138.58197E	299.797	5.2
99-11-16	21:51:51.392	42.27517N	138.01109E	315.249	5.0
99-12-03	02:52:00.998	45.82316N	141.79452E	49.354	5.0
99-12-05	16:28:32.227	42.48970N	139.22130E	232.585	6.0
99-12-12	05:24:27.191	40.08658N	145.39787E	96.184	5.4
		Local Earthquakes			
Western cluster					
99-07-01	07:13:38.209	42.21057N	142.74188E	31.801	3.2
99-07-18	02:20:28.144	42.21075N	142.58448E	57.290	4.1
99-08-16	07:32:40.622	42.19958N	142.89189E	57.843	4.5
99-11-24	10:49:52.359	42.13535N	142.90984E	42.201	3.1
99-12-05	10:50:16.437	42.12799N	142.77987E	52.687	3.1
99-12-19	00:01:59.194	42.27426N	142.61304E	52.537	3.3
Eastern cluster					
99-07-23	04:10:23.949	42.24003N	143.87531E	51.385	3.1
99-08-14	08:55:05:982	42.14487N	143.83058E	55.215	2.9
99-08-30	01:19:51.051	42.14116N	143.79197E	55.169	3.3
99-09-22	21:33:44.925	42.24739N	143.80548E	55.207	2.9
99-11-23	03:16:41.967	42.31248N	143.94888E	61.215	3.3
99-11-28	13:56:08.723	42.30541N	143.95134E	59.611	2.7

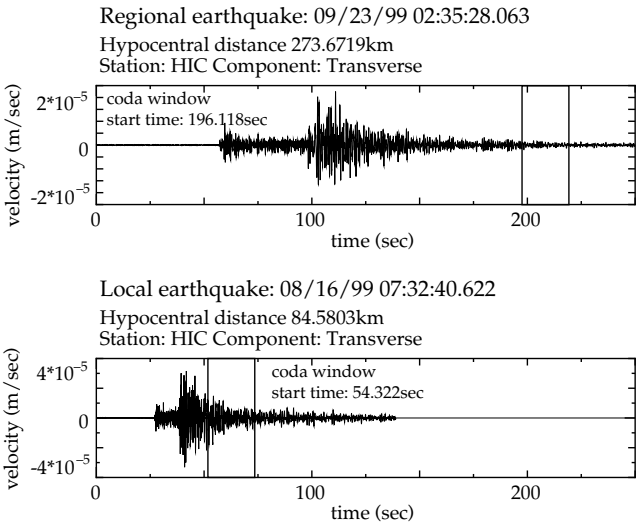

Figure 3. Example of seismograms at different hypocentral distances. Black lines indicate the time windows to be analyzed.

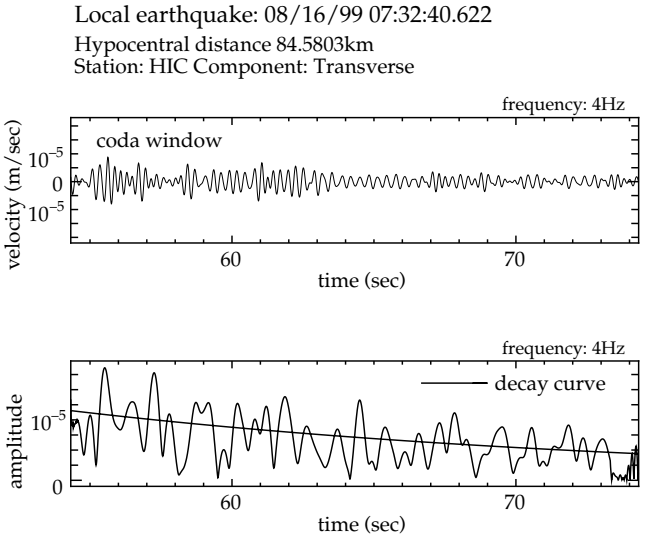

Figure 4. Example of a bandpass-filtered seismogram and envelope after the correction of the geometrical spreading factor, together with the estimated decay curve of coda.

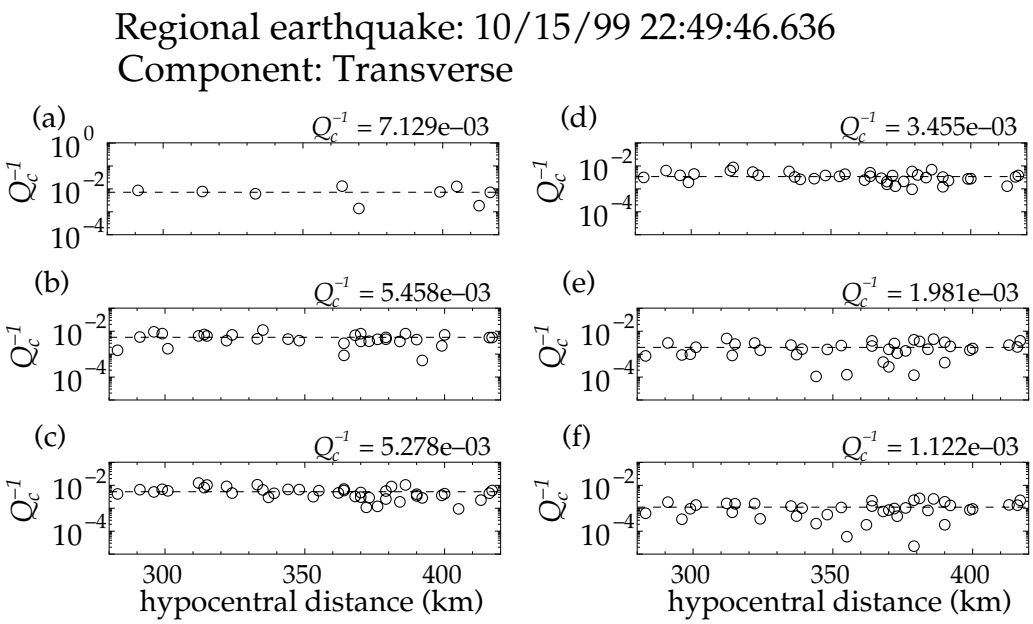

Figure 5. Q_c^{-1} versus stations in the transverse component for the regional earthquakes, 15 October 1999, at six frequency bands: (a) 1, (b) 2, (c) 4, (d) 8, (e) 16, and (f) 32 Hz.

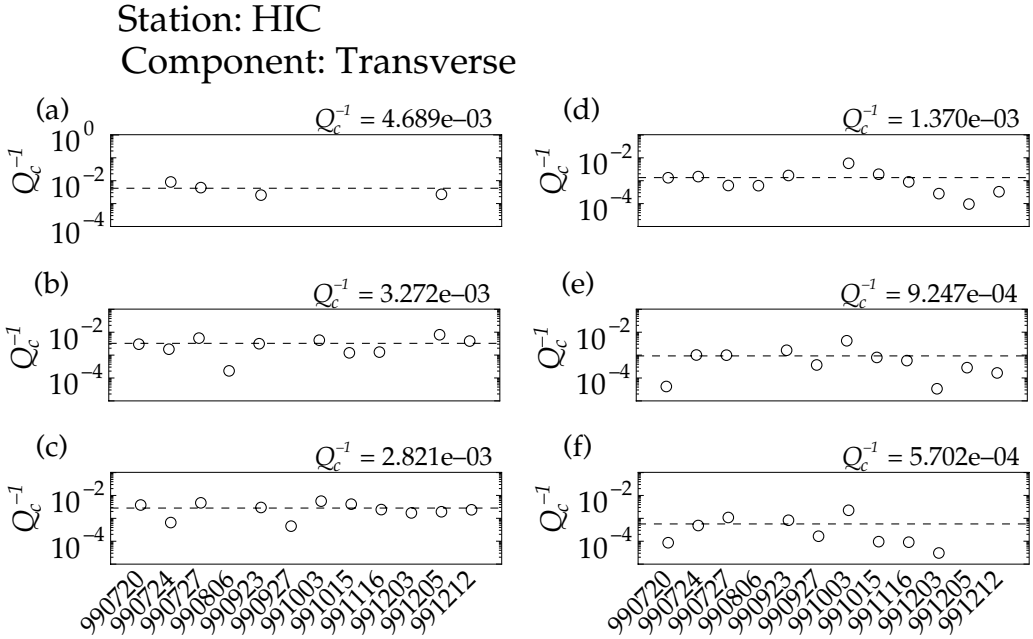

Figure 6. Q_c^{-1} versus regional earthquakes in the transverse component at station HIC at six frequencies: (a) 1, (b) 2, (c) 4, (d) 8, (e) 16, and (f) 32 Hz.

as obtained in the previous section, should be nearly constant among all source–station pairs. Recent careful studies have clearly shown that coda levels fluctuate significantly and systematically within a dense seismic network (e.g., Aki and Ferrazzini, 2000). In such a case, the assumption used in the previous section, that is, $C_{ij}(f, t) \simeq \tilde{C}_{ij}(f, t)$ in equation (2), becomes no longer valid. In order to evaluate such fluctuations of coda levels, we estimate coda amplitudes, after correcting for the RSAF, for local earthquakes occurring in the neighborhood of stations.

We define a relative coda amplification factor (CAF) as the ratio of the coda level $A_{oj}(f, t)$ for the oth local earthquake at the jth station to the average $\tilde{A}_o(f, t)$ over all the stations, after the correction of $\mathrm{RSAF}_j(f)$:

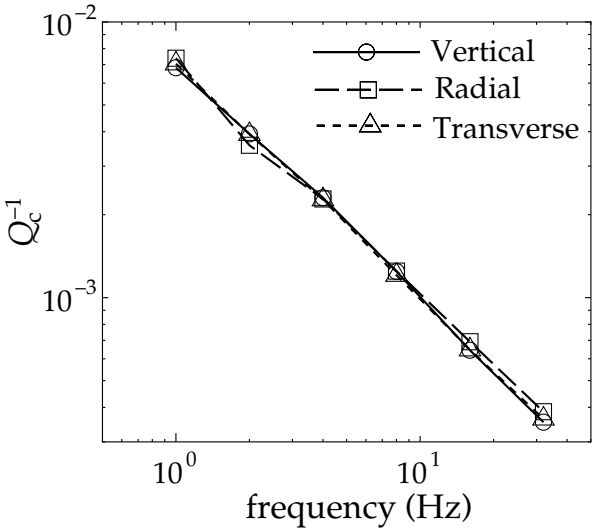

Figure 7. Frequency dependency of Q_c^{-1} of three components averaged over all the regional earthquakes and the stations.

$$\mathrm{RSAF}_j^{-1}(f) \times \frac{A_{oj}(f,\ t)}{\tilde{A}_o(f,\ t)} = \frac{S_o(f) \cdot C_{oj}(f,\ t)}{S_o(f) \cdot \tilde{C}_o(f,\ t)} = \frac{C_{oj}(f,\ t)}{\tilde{C}_o(f,\ t)} \equiv \mathrm{CAF}_j(f), \quad (5)$$

where S_o is the source term of the oth local earthquake. $C_{oj}(f,\ t)$ and $\tilde{C}_o(f,\ t)$ are the averaged propagation or path terms for the jth station and that averaged over all the stations, respectively. CAF values correspond to the average values of coda level over this time window. Since we use a relatively large lapse time of coda (i.e., greater than twice the S-wave travel time), the term $C(f,\ t)$ is assumed to be expressed as equation (4). The ratio in the second right of equation (5) does not depend on time, and it indicates the overall pattern of spatial distribution of small-scale heterogeneities. If heterogeneities are distributed uniformly in space, $\mathrm{CAF}_j(f)$ should be unity, as assumed and confirmed for regional earthquakes in the previous section [i.e., $C_{ij}(f,\ t) \simeq \tilde{C}(f,\ t)$]. If $\mathrm{CAF}_j(f) \gg 1$, heterogeneities are supposed to be localized in regions between the oth local earthquake and the jth station.

We analyzed three-component seismograms for 12 local earthquakes, as shown in Figure 2. Figure 9 shows the spatial distribution of CAF values in the transverse component at each frequency (1–32 Hz) for local earthquakes to the west of the Hidaka Mountains in the left, and the right for those in the east. We found a strong dependency of CAF values on locations of source–station pairs at every frequency band, which means that small-scale heterogeneities in this region should be far from uniformly distributed. As an overall feature, CAF values are relatively high in a low-frequency range (1–2 Hz) at stations in the western part of the Hidaka region, particularly ATU and HYK (>2.3 times), implying the possibility of concentrated heterogeneities in the western part, as a locally large degree of scattering. On the other hand, CAF values in a frequency range of higher than 16 Hz are relatively large if a path traverses the Hidaka Mountains (Fig. 9e,f). That is, large CAF values are found at eastern stations for local earthquakes to the west of the Hidaka Mountains, as well as at western stations for local earthquakes in the east. The distribution of the CAF at intermediate frequency (4 and 8 Hz) does not show any specific anomalies, while there are several systematic patterns at both low (<2 Hz) and high (>16 Hz) frequencies.

Spatial Distribution of Heterogeneities in the Hidaka Region

In the previous section, we identified the nonuniform spatial distribution of small-scale heterogeneities by using CAF values and found that small-scale heterogeneities in the Hidaka region should be distributed not only in a nonuniform manner but also with different scale length, estimated from their frequency dependence.

Recently, Revenaugh (1995) applied the Kirchhoff coda migration method to teleseismic P coda waves in the upper mantle beneath the Southern California Seismic Network, stacking these data as the energy of single-scattered waves. He showed an area of strong scattering in an edge of a subducting slab as a sharp thermal boundary. Such a boundary could be produced by heating of the slab or small-scale convection in the surrounding mantle. Matsumoto *et al.* (1999) proposed another method, called slant stacking, showing that strong scatterers are distributed around the fault plane of the 1896 Rikuu, Japan, earthquake, located in the midcrust to lowercrust. They interpreted that the distribution of scatterers in the upper crust is correlated to the hypocenter distribution of microearthquakes. In contrast, Nishigami (1997) applied the recursive stochastic inversion to obtain the distribution of scatterers in two volcanic regions and one active-fault region in the central part of Japan. He estimated detailed distributions of S-wave reflectors beneath active volcanoes such as Mounts Ontaka and Nikko-Shirane. He also found an area of weak scattering correlated with a seismic gap in the Hokuriku region. Tsuruga *et al.* (2003) estimated the spatial distribution of small-scale heterogeneities in and around the Hanshin–Awaji region, including the coseismic fault region of the 1995 Hyogo-ken Nanbu earthquakes by a method similar to this study. They found strong heterogeneities with a scale of 0.2–1.4 km located around the depth of 10 km along the Nojima fault.

Yomogida *et al.* (1997) studied scattered waves by localized heterogeneities with numerical simulations, focusing on the spatial variation of coda levels relative to focal depth in media where heterogeneities are localized within a certain depth range. They suggested that the notable local amplification of coda takes place only in a particular frequency range in which the scattering effect is the strongest: the nondimensional frequency kd, (wave number) × (size of each

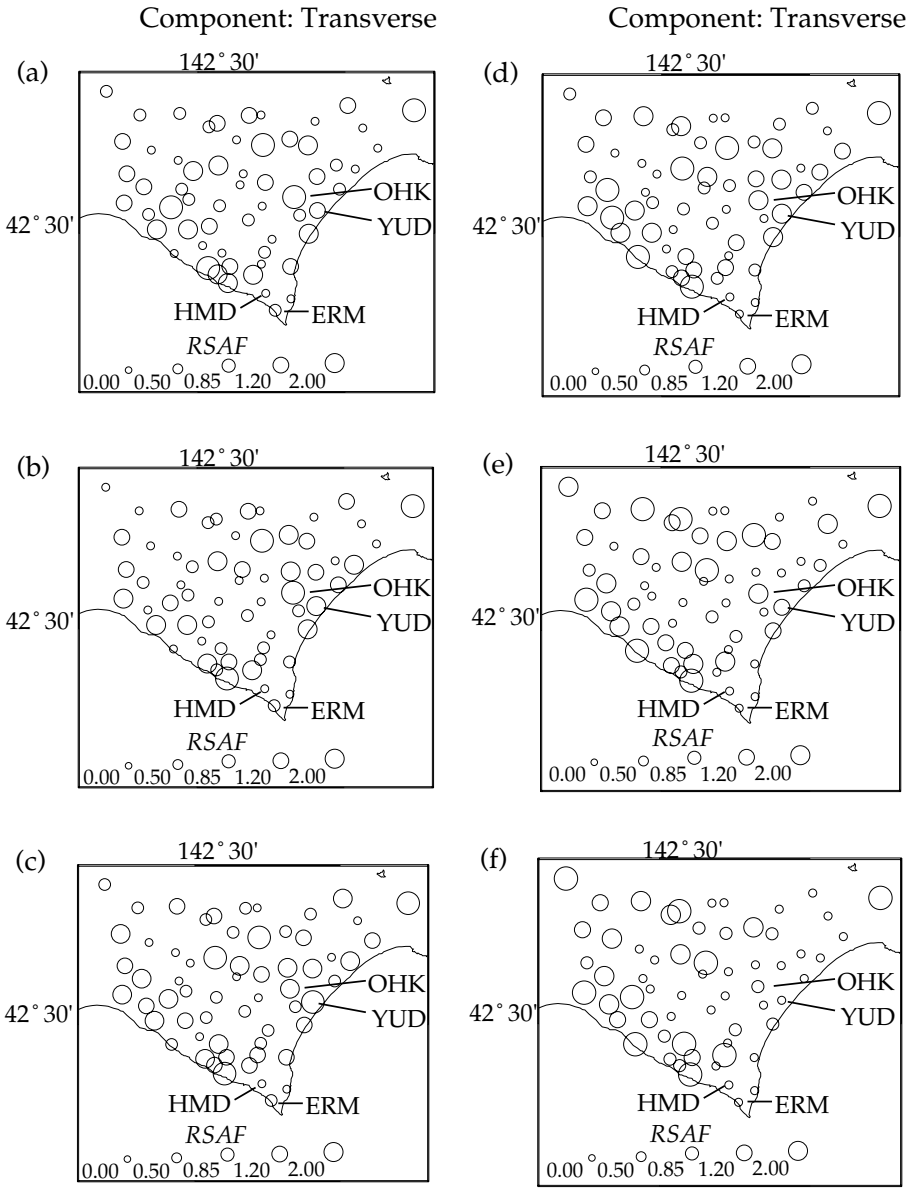

Figure 8. Distribution of relative site amplification factors (RSAFs) in the transverse component at stations in frequency bands of (a) 1, (b) 2, (c) 4, (d) 8, (e) 16, and (f) 32 Hz.

heterogeneity), is about 2. Using their result, the corresponding scale of each heterogeneity in the western part is estimated to be about 0.6–1.3 km because of the observed dominant frequency range of 1–2 Hz, assuming the shear-wave velocity to be 4.0 km/sec (Suzuki *et al.*, 1988). CAF values at 1 and 2 Hz are large at many stations (e.g., ATU and HYK in Fig. 9a,b) in the west of the Hidaka Mountains, regardless of earthquake locations. This result implies the existence of localized heterogeneities near these stations, as schematically shown in Figure 10a. Figure 11 shows the distribution of microearthquakes (magnitude <4, depth <30 km) and CAF values for the eastern cluster earthquakes in the transverse component at 1 Hz. The distribution of the CAF in low frequency (<2 Hz) appears to agree with the shallow seismic activity (<30 km) in this region. This may correspond to an area of highly concentrated heterogeneities of the size around 0.6–1.3 km, attributing to the high activity of microearthquakes.

Let us discuss the high-frequency CAF pattern in the high-frequency range (>16 Hz), as shown in Figure 9e,f. In this range, the heterogeneities should be on a characteristic scale less than 0.1 km, using the assumption of single as well as isotropic scattering and the maximum scattering taking place at $kd \simeq 2$. From the adopted lapse time of coda (i.e., about 65 sec), we can estimate the location of the origin of this CAF anomaly by calculating the length of a ray path

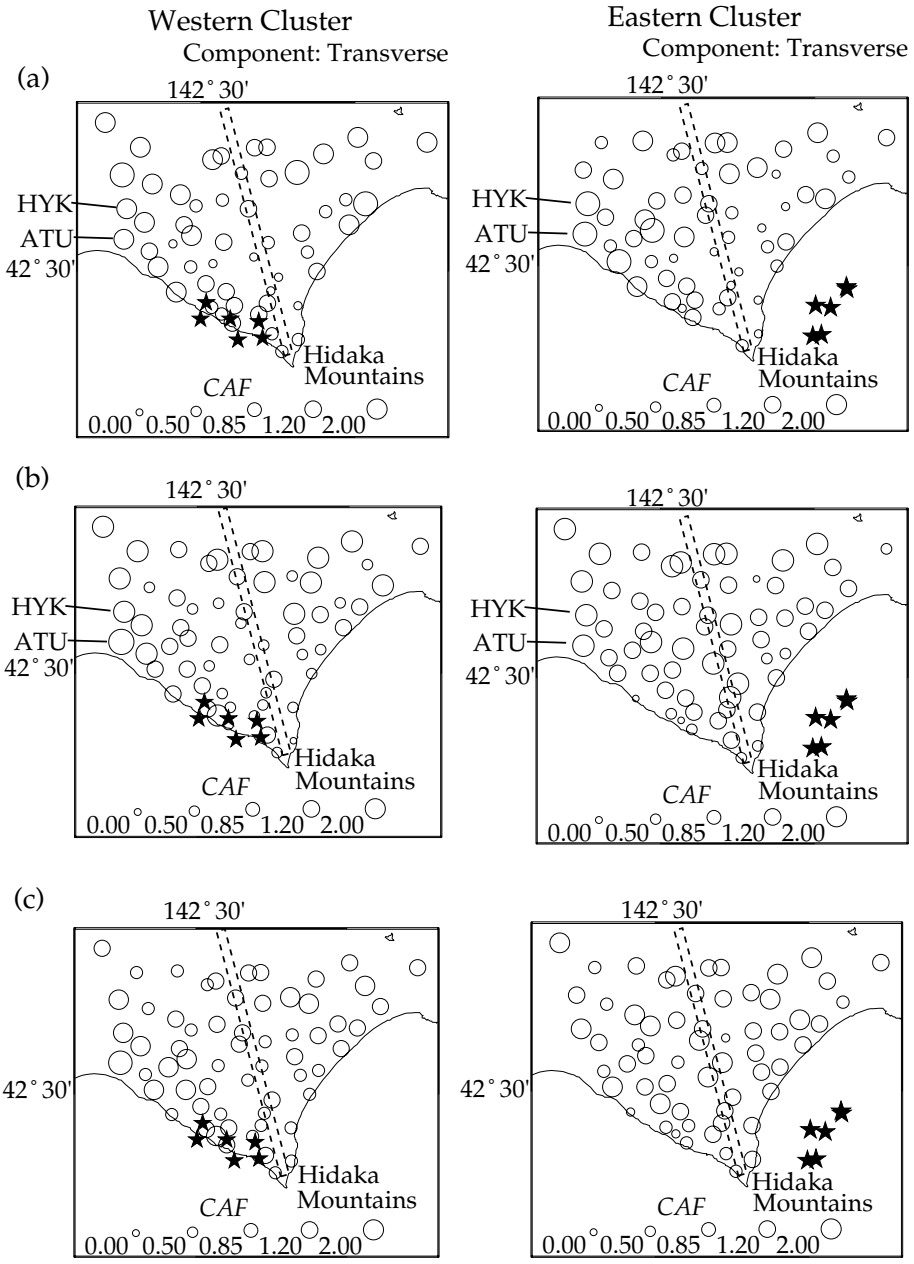

Figure 9. Distribution of the CAF in the transverse component for local earthquakes in the western Hidaka region (left) and those in the eastern Hidaka region (right) in frequency bands of (a) 1, (b) 2, (c) 4, (d) 8, (e) 16, and (f) 32 Hz.

in a constant-velocity medium (*S* wave to be 4.0 km/sec) with the single-scattering model (Fig. 10b). This result thus can be explained by the existence of a zone with concentrated heterogeneities beneath the Hidaka Mountains at the depth of 100–120 km. Nevertheless, the observed pattern of large CAF values in Fig. 9e,f cannot be clearly applied to such a simple model of isotropic scattering because isotropic scattering should radiate waves to every station but not specific ones, as in this case. This region of these heterogeneities is most likely to correspond to an internal part of the subducting Pacific plate beneath this region (Katsumata *et al.*, 2001b), as shown by a black line in Figure 12. This result implies a thin and flat zone of many small (<0.1 km) heterogeneities, behaving as a strong reflection interface there, such as observed in the Kanto district by Obara and Sato (1995).

Conclusions

We investigated small-scale heterogeneities in the Hidaka region from spatial variations of coda envelope recorded by a dense seismic array. We analyzed three-

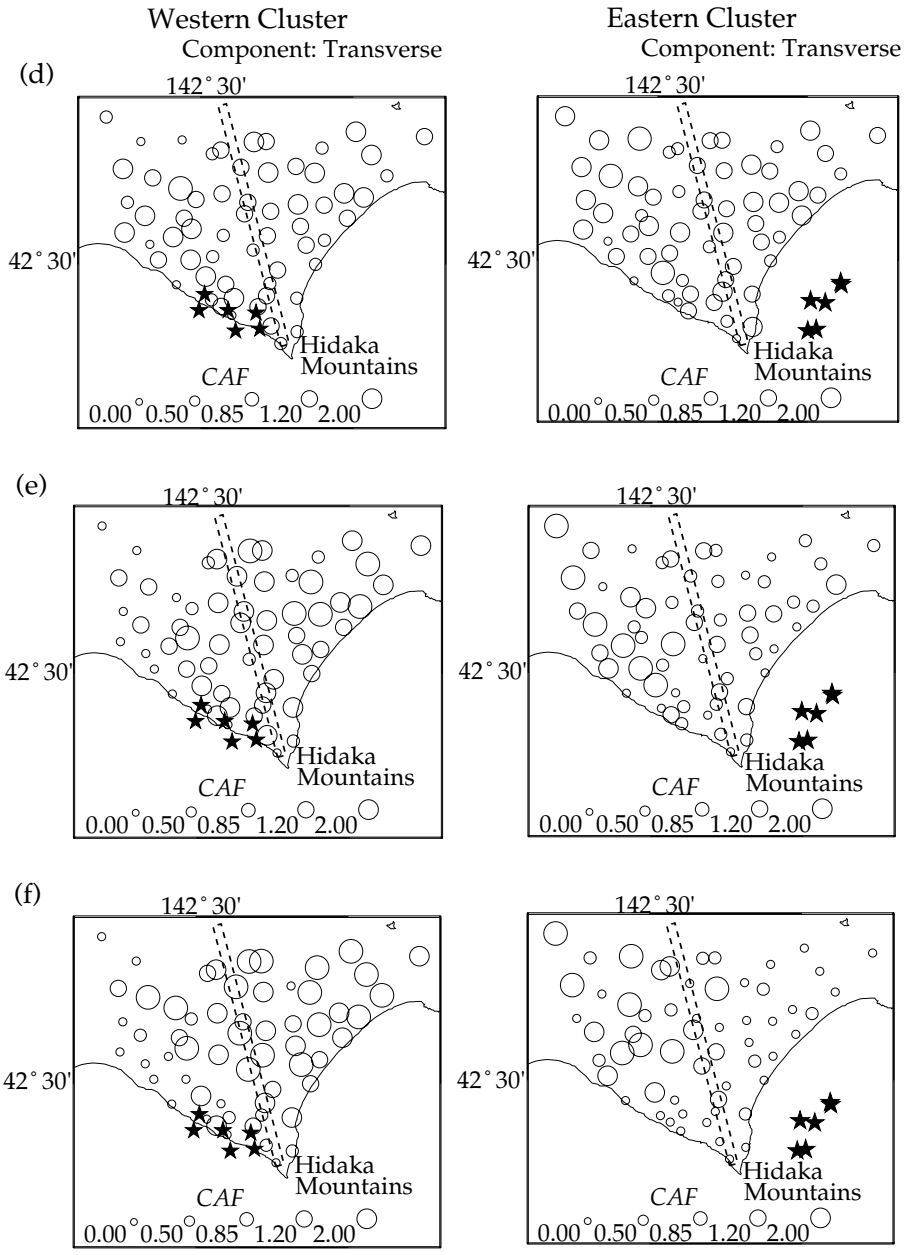

Figure 9. Continued.

component seismograms in frequency ranges from 1 to 32 Hz. We first estimated the site amplification factor at each station using 12 regional earthquakes of large epicentral distances. After the correction of such a site effect, we obtained the coda wave amplitude of each source–station pair for 12 local earthquakes and found systematic variations of coda wave amplitude anomalies. This result strongly suggests a nonuniform distribution of small-scale heterogeneities in this region.

We revealed the following remarkably nonuniform distribution of CAF in the Hidaka region:

1. CAF values are large in the west of the Hidaka Mountains only at low frequency (<2 Hz). This large CAF area agrees with an area of high microearthquake seismisity, and there may exist highly concentrated fractures with the characteristic size of 0.6–1.3 km, estimated from its observed frequency.
2. Strong heterogeneities with a scale less than 0.1 km may be located at a deep part (100–120 km) beneath the Hidaka Mountains. Such a zone of strong scattering appears to correspond to a heterogeneous zone inside the subducting Pacific plate. These small (<0.1 km) heterogeneities behave as a strong seismic reflector for high-frequency seismic waves.

We have obtained images of scatterer that are useful in elucidating small-scale heterogeneous structures of the

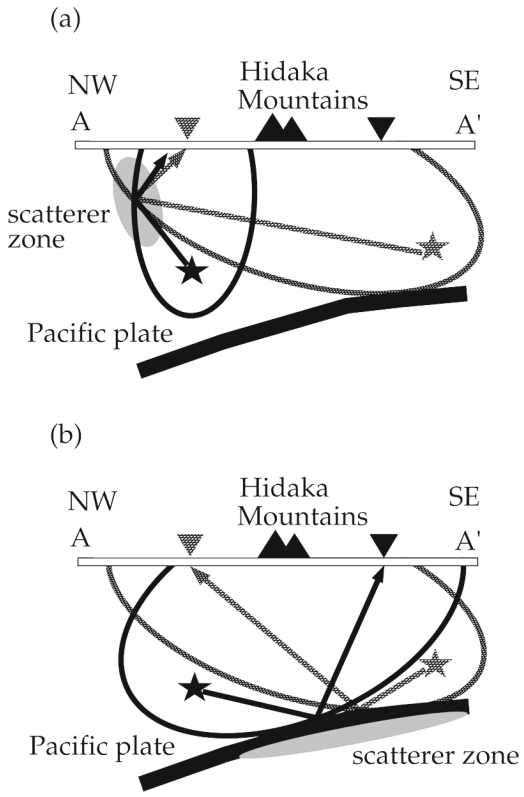

Figure 10. Schematic illustration showing the frequency dependence scatterers for some sets of stations and earthquakes plotted on the cross-sectional view of the Pacific plate in (a) low (<2 Hz) and (b) high (>16 Hz) frequencies.

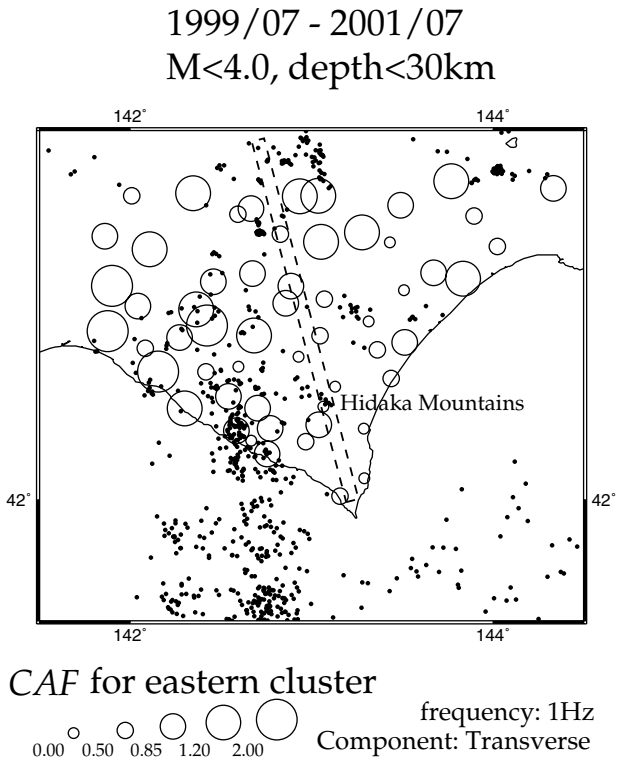

Figure 11. Epicenter distribution of shallow (M <4, depth < 30 km) earthquakes that occurred in central Hokkaido during the period from July 1999 to July 2001. Open circles denote the CAF for the eastern cluster shown in Figure 9a.

Hidaka region. This study employed several assumptions on the scattering process and velocity structure. Further advanced analysis will be required to interpret physical features of the heterogeneous structure in this region in a more quantitative manner by introducing both a more realistic scattering process and velocity structure.

Acknowledgments

We thank Professors Junji Koyama, Takeo Moriya, and Yoshinobu Motoya at Hokkaido University for their encouragement and helpful advice. We also thank Naoto Wada at Hokkaido University and Takashi Mizuno at Kyoto University for their help in processing the seismic records used in this study. We also wish to thank Drs. Kei Katsumata and Ryou Honda at Hokkaido University for their constructive comments. Valuable comments by Professor Kin'ya Nishigami at Kyoto University, two anonymous reviewers, and the *Bulletin* editor are greatly appreciated. We are grateful to the Research Group of Hidaka Collision Zone for permission to use their seismic waveform data and to the members of its analyzing committee for the preparation of the data. The observation was conducted by Hokkaido University, Tohoku University, the Earthquake Research Institute, University of Tokyo, Nagoya University, Disaster Prevention Research Institute Kyoto University, and Kyushu University as a part of the new Program of the Study and Observation for Earthquake Prediction. We also used seismic waveform data and hypocentral parameters provided by the Institute of Seismology and Volcanology, Hokkaido University. Further thanks are given to Ken Otsuka and Wakana Matsubara at Hokkaido University for their useful suggestions during this study. This research was partially supported by the Earthquake Research Institute Cooperative Research Program (2000-B-07).

References

Aki, K. (1969). Analysis of seismic coda of local earthquakes as scattered waves, *J. Geophys. Res.* **74,** 615–631.

Aki, K., and B. Chouet (1975). Origin of coda waves: source, attenuation, and scattering effects, *J. Geophys. Res.* **80,** 3322–3342.

Aki, K., and V. Ferrazzini (2000). Seismic monitoring of an active volcano for prediction, *J. Geophys. Res.* **105,** 16,617–16,640.

Iyer, H. M., and K. Hirahara (Editors) (1993). *Seismic Tomography: Theory and Practice*, Chapman and Hall, London, 842 pp.

Katsumata, K., N. Wada, and M. Kasahara (1999). Near real-time seismic tomography, *Prog. Abstr. Seism. Soc. Japan* B43 (in Japanese).

Katsumata, K., N. Wada, and M. Kasahara (2001a). Seismotectonics in the Hidaka collision zone, Hokkaido, Japan, *Prog. Abstr. Seism. Soc. Japan* B60 (in Japanese).

Katsumata, K., N. Wada, and M. Kasahara (2001b). Pull-apart fracture zone inside the deep Pacific plate discovered by a new dense seismic network, *Geophys. Res. Lett.* (submitted).

Matsumoto, S., K. Obara, and A. Hasegawa (1998). Imaging *P*-wave scatterer distribution in the focal area of the 1995 *M* 7.2 Hyogo-ken Nanbu (Kobe) earthquake, *Geophys. Res. Lett.* **25,** 1439–1442.

Matsumoto, S., K. Obara, K. Yoshimoto, T. Saito, A. Hasegawa, and A. Ito (1999). Imaging of inhomogeneous structure of the crust beneath Ou backbone range, Northeastern Japan, based on small aperture seismic array observations, *J. Seism. Soc. Japan Ser. 2* **52,** 283–297 (in Japanese with English abstract).

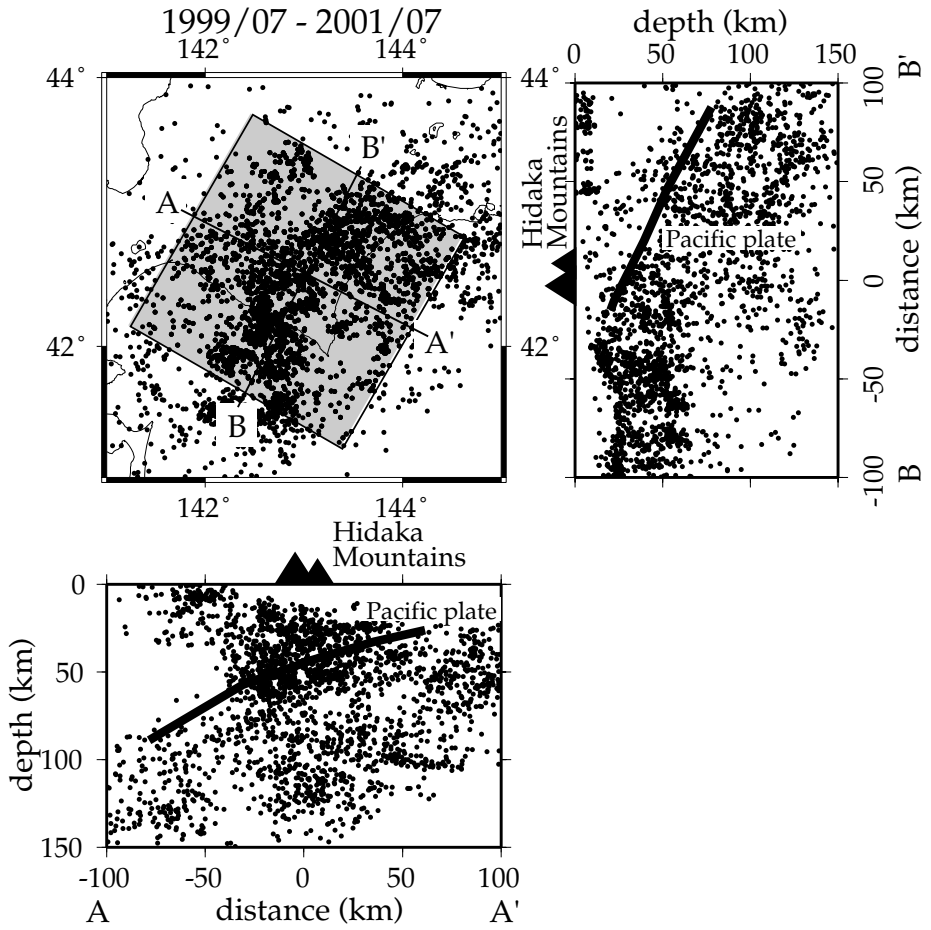

Figure 12. Hypocenter distribution in and around Hokkaido during the period from July 1999 to July 2001. Black lines correspond to the upper interface of the subducting Pacific plate (Katsumata *et al.*, 2001b).

Moriya, T., H. Miyamachi, O. Ozel, N. Ozel, T. Iwasaki, and M. Kasahara (1997). Collision structure and seismotectonics of the Hidaka Mountains, Hokkaido, Japan, *Struct. Geol.* **42,** 15–30 (in Japanese with English abstract).

Moriya, T., H. Okada, T. Matsushima, S. Asano, T. Yoshii, and A. Ikami (1998). Collision structure in the upper crust beneath the southwestern foot of the Hidaka Mountains, Hokkaido, Japan, as derived from explosion seismic observations, *Tectonophysics* **290,** 181–196.

Nishigami, K. (1991). A new inversion method of coda waveforms to determine spatial distribution of coda scatterers in the crust and uppermost mantle, *Geophys. Res. Lett.* **18,** 2225–2228.

Nishigami, K. (1997). Spatial distribution of coda scatterers in the crust around two active volcanoes and one active fault system in central Japan: inversion analysis of coda envelopes, *Phys. Earth Planet. Interiors* **104,** 75–89.

Obara, K., and H. Sato (1995). Regional differences of random inhomogeneities around the volcanic front in the Kanto–Tokai area, Japan, revealed from the broadening of *S* wave seismogram envelopes, *J. Geophys. Res.* **100,** 2103–2121.

Phillips, W. S., and K. Aki (1986). Site amplification of coda waves from local earthquakes in central California, *Bull. Seism. Soc. Am.* **76,** 627–648.

Revenaugh, J. (1995). A scattered-wave image of subduction beneath the Transverse Range, California, *Science* **268,** 1888–1892.

Sato, H., and M. C. Fehler (1998). *Seismic Wave Propagation and Scattering in the Heterogeneous Earth*, Springer, New York, 308 pp.

Suzuki, S., T. Takanami, Y. Motoya, and I. Nakanishi (1988). A real-time automatic processing system of seismic waves for the network of Hokkaido university, *J. Seism. Soc. Japan Ser. 2* **41,** 359–373 (in Japanese with English abstract).

Takahara, M., and K. Yomogida (1992). Estimation coda *Q* using the maximum likelihood method, *Pageoph* **139,** 255–268.

Tsuruga, K., K. Yomogida, H. Ito, and K. Nishigami (2003). Detection of Localized Small-Scale Heterogeneities in the Hanshin-Awaji Region, Japan, by Anomalous Amplification of Coda Level, *Bull. Seism. Soc. Am.* **93,** 1516–1530.

Yomogida, K., R. Benites, P. M. Roberts, and M. Fehler (1997). Scattering of elastic waves in 2-D composite media. II. Waveforms and spectra, *Phys. Earth Planet. Interiors* **104,** 175–192.

Division of Earth and Planetary Sciences
Graduate School of Science
Hokkaido University
North 10 West 8
Kita-ku, Sapporo 060-0810, Japan
taka@noreply.ep.sci.hokudai.ac.jp.

Manuscript received 1 March 2002.